

Aug 22th. 2024

Quark deconfinement in neutron stars by Color-Molecular-Dynamics

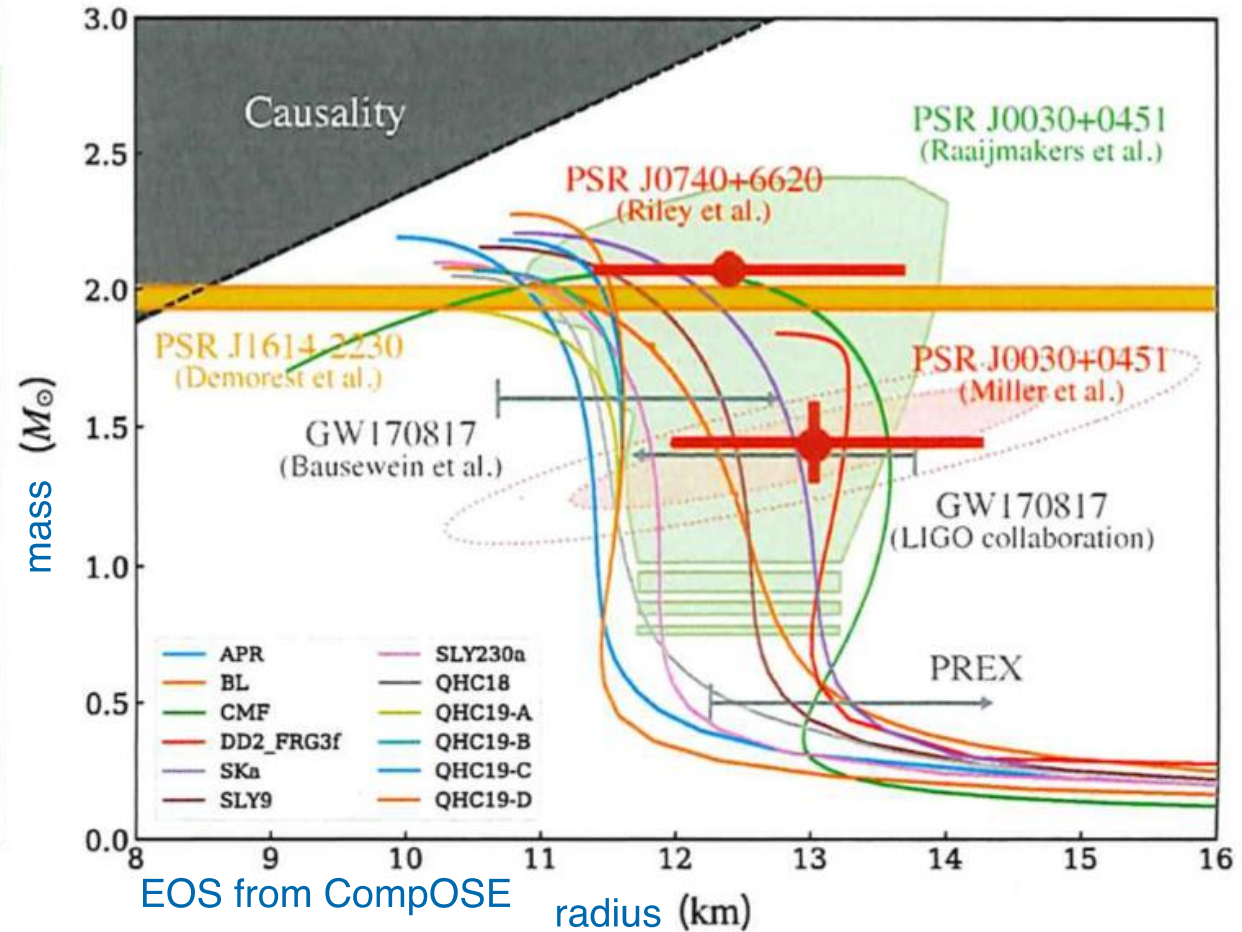
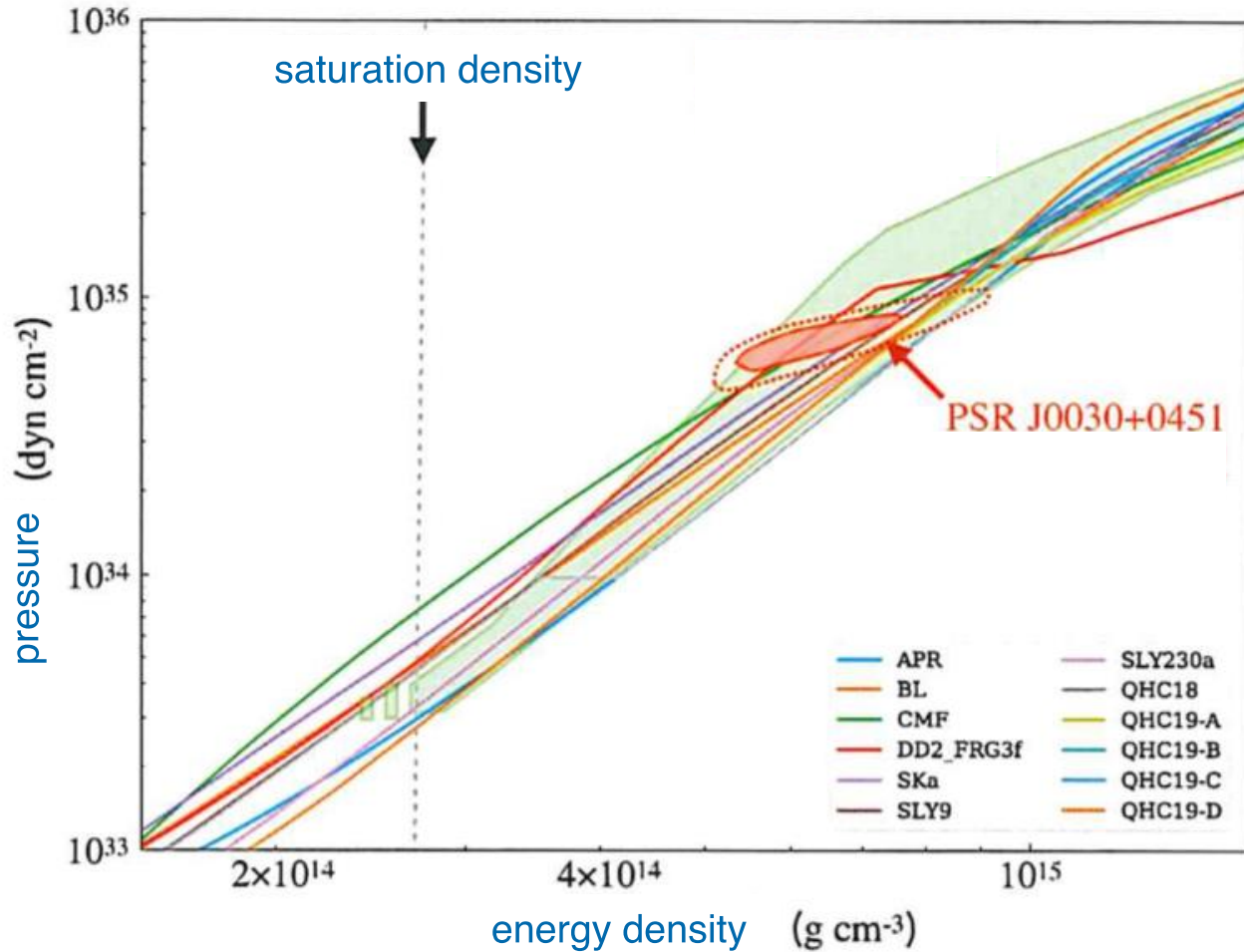
N. Yasutake (Chiba Inst. Tech./JAEA)

T.Maruyama(JAEA)

PRD 109. 043056 (2024)

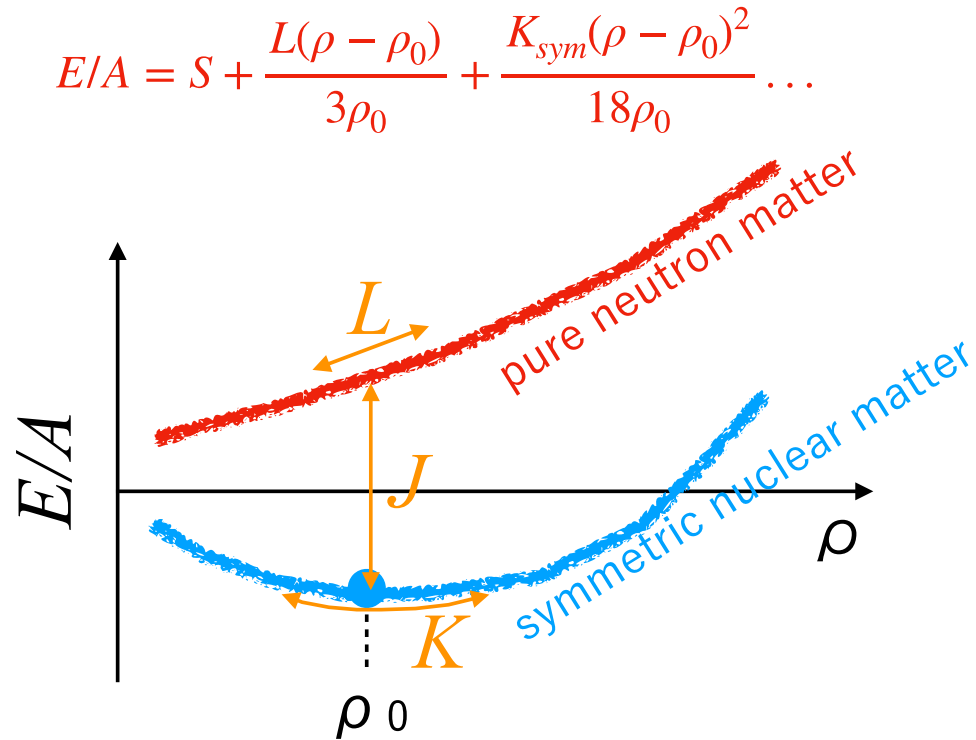
EOS and M-R relation

Enoto & NY (2021) Oct. Journal of Japanese Physical Society

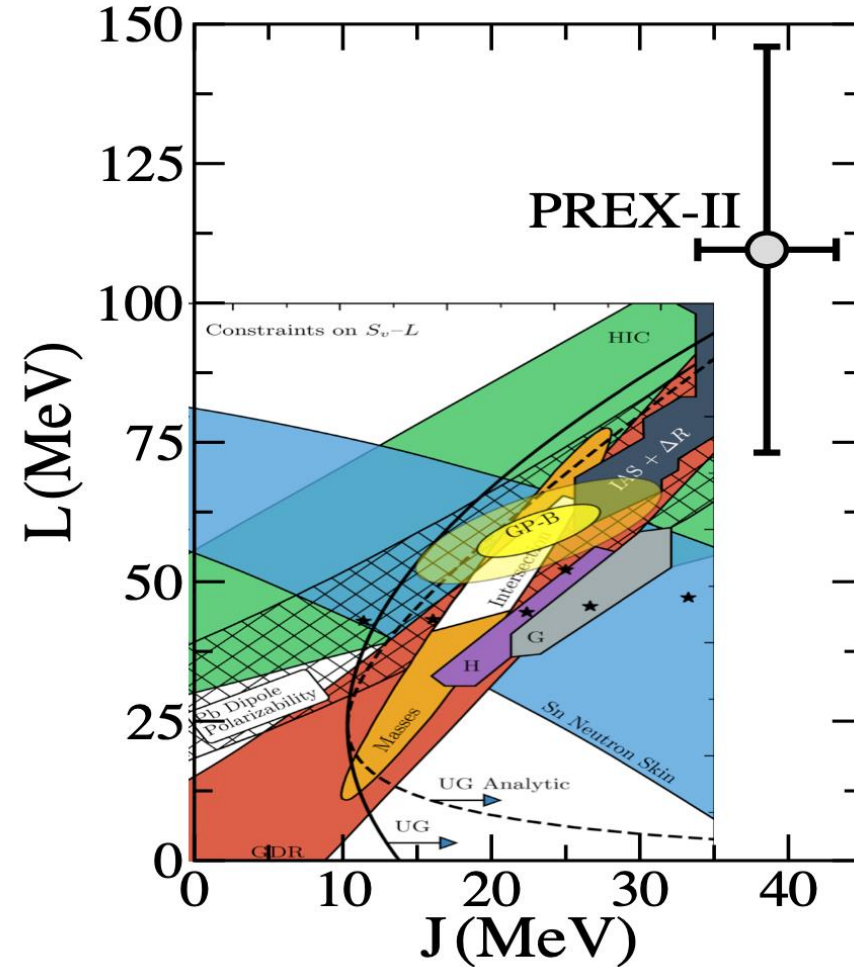


EOS Constraints around saturation density

Reed et al. PRL 126,172503 (2021)

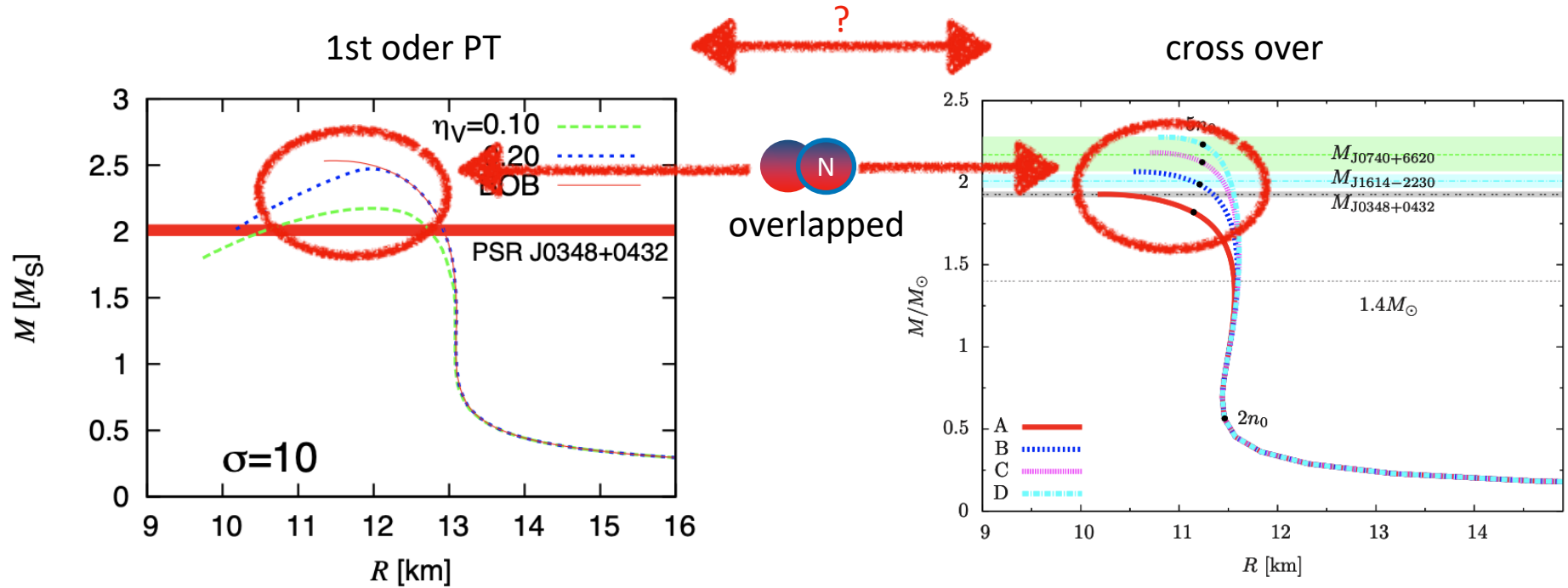


$$E/A = S_0 + \frac{K(\rho - \rho_0)^2}{18\rho_0^2} \dots$$



- The result of PREX-II depends on the analysis methods. (Reinhard et al. PRL 127.232501(2021))
- **CREX** results suggest ordinary L values, not large as PREX-II. (Adhikari et al. PRL 129.042501(2022))

EOS from quarks to neutron stars



NY, et al. PRC 90, 067302 (2014)

G. Baym, et al. ApJ 885, 42 (2019)

nucleon(BHF model) + quark(eNJL model)

nucleon(Variational method) + quark(NJL model)

See also Xia, Maruyama, NY, Tatsumi, Shen, Togashi (2020), Phys. Rev. D 102, 023031

Problems

① How much can we believe hadron models at high density region?

② 1st order or cross over?

→ It is dependent on the assumption (not results).

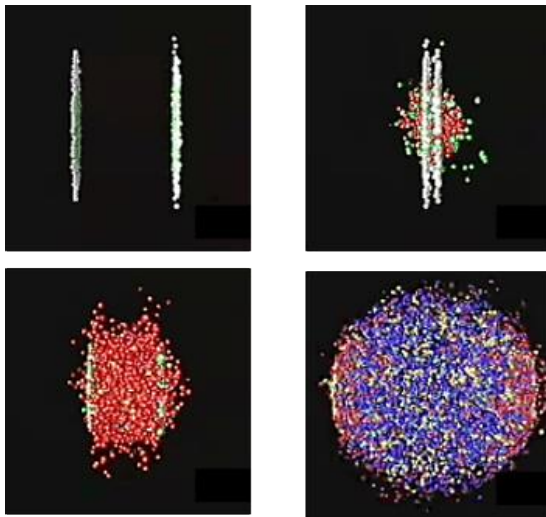
→ We can not get unified understanding.

cf.) We can not obtain the other physical properties for crossover.

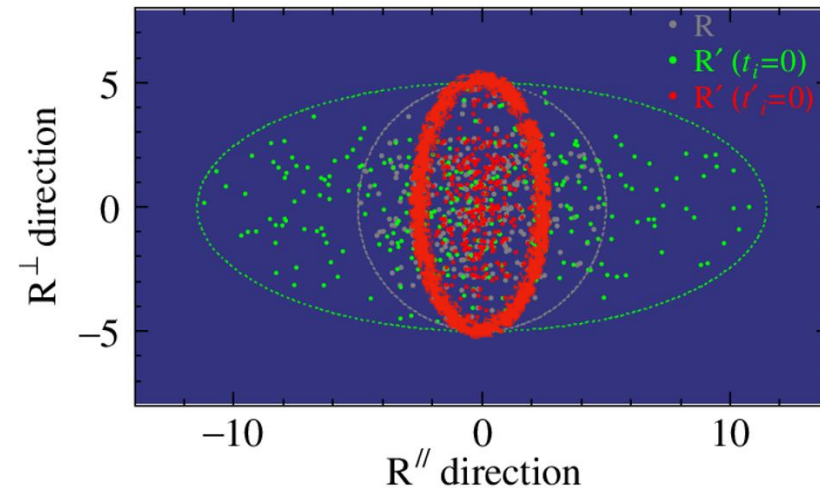
Molecular dynamics

Why molecular dynamics ?

- ① We focus on Quark-Molecular-Dynamics.
→ We can describe EOS and NS physics only with quark system.
- ② MD enables us to know also dynamical behaviors, fluctuation, clustering.
→ We can apply MD directly to Heavy Ion Collisions.



UrQMD for RHIC
<https://www.bnl.gov/rhic/physics.php>



Relativistic color molecular dynamics
(on going project)

Formulation

NY, Maruyama (2024) PRD
Maruyama, Hatsuda (2000) PRD

number of variables

$$\{x, y, z, Px, Py, Pz, \alpha, \beta, \theta, \varphi\}_i$$

10 variables on each particle

wave functions

$$\Psi = \prod_{i=1}^{3A} \phi_i(\mathbf{r}) \chi_i \quad \chi_i = f_i s_i c_i$$

f_i ... flavors (fixed)

s_i ... spins (fixed. But unfixed later section) \uparrow or \downarrow

$$c_i \equiv \begin{pmatrix} \cos \alpha_i e^{-i\beta_i} \cos \theta_i \\ \sin \alpha_i e^{+i\beta_i} \cos \theta_i \\ \sin \theta_i e^{i\varphi_i} \end{pmatrix} \begin{matrix} \text{R} \\ \text{G} \\ \text{B} \end{matrix}$$

$$\phi_i(\mathbf{r}) \equiv (\pi L^2)^{-\frac{3}{4}} \exp[-(\mathbf{r} - \mathbf{R}_i)^2 / 2L^2 - i\mathbf{P}_i \mathbf{r}]$$

time evolution

$$\frac{\partial \mathcal{L}}{\partial q} = \frac{d}{dt} \frac{\partial \mathcal{L}}{\partial \dot{q}} \quad \mathcal{L} = \left\langle \Psi \left| i\hbar \frac{d}{dt} - \hat{H} \right| \Psi \right\rangle$$

cooling

$$\begin{aligned} \dot{\mathbf{R}}_i &= \frac{\partial H}{\partial \mathbf{P}_i} + \mu_R \frac{\partial H}{\partial \mathbf{R}_i}, \\ \dot{\mathbf{P}}_i &= -\frac{\partial H}{\partial \mathbf{R}_i} + \mu_P \frac{\partial H}{\partial \mathbf{P}_i}, \end{aligned}$$

confinement conditions

$$\begin{cases} |\mathbf{R}_i - \mathbf{R}_j| < d_{cluster} & (i, j = 1, 2, 3) \\ \sum_{a=1}^8 \left[\sum_{i=1}^3 \langle \chi_i | \lambda^a | \chi_i \rangle \right]^2 < \varepsilon \end{cases}$$

λ^a being the Gell-Mann matrices

Interactions

The system follows the Hamiltonian,

$$H = H_0 + V_{\text{Pauli}} - T_{\text{spur}},$$

where H_0 is the conventional Hamiltonian expressed as

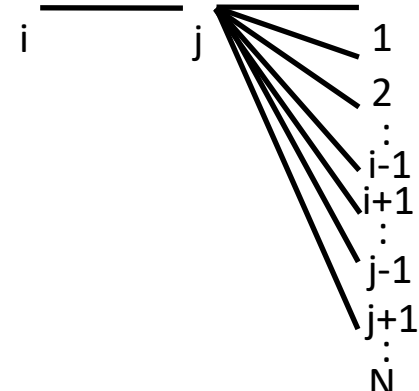
$$H_0 = \left\langle \Psi \left| \sum_{i=1}^N \sqrt{m + \hat{\mathbf{p}}_i^2} + \frac{1}{2} \sum_{i,j \neq i} \hat{V}_{ij} \right| \Psi \right\rangle.$$

$$\hat{V}_{i,j} = - \sum_{a=1}^8 \tau_i^a \tau_j^a \hat{V}_C + \hat{V}_M, \quad \tau_i^a = \lambda_i^c / 2 \text{ with } \lambda_i^c \text{ being the Gell-Mann matrices.}$$

$$\hat{V}_C = \kappa \hat{r}_{ij} - \frac{\alpha_s}{\hat{r}_{ij}},$$

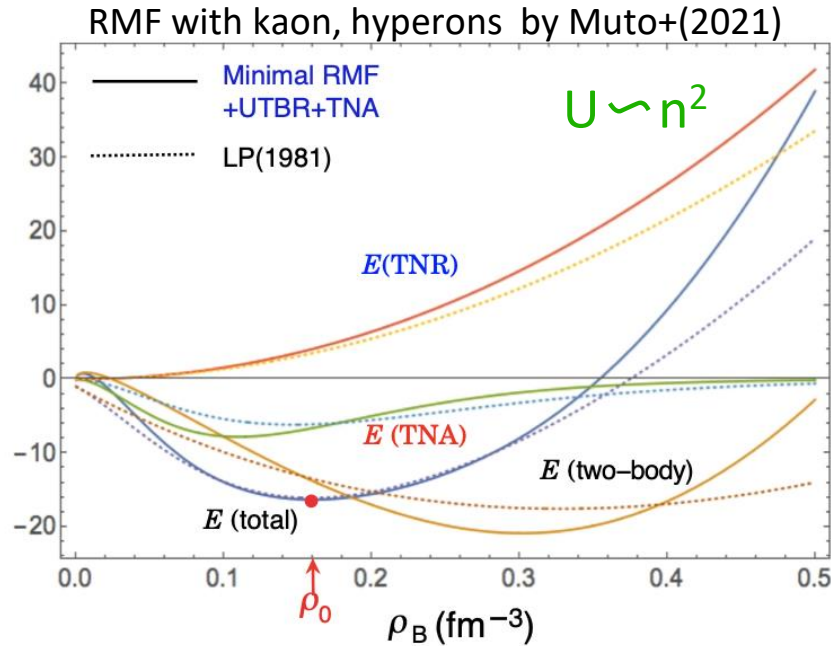
$$\hat{V}_M = \frac{g_\omega^2 C_\omega}{4\pi} \left(\sum_{j \neq i}^n \frac{e^{-\mu_\omega \hat{r}_{ij}}}{\hat{r}_{ij}} \right)^{1+\epsilon_\omega} - \frac{g_\sigma^2 C_\sigma}{4\pi} \left(\sum_{j \neq i}^n \frac{e^{-\mu_\sigma \hat{r}_{ij}}}{\hat{r}_{ij}} \right)^{1+\epsilon_\sigma} + \frac{\sigma_i^3 \sigma_j^3}{4} \frac{g_\rho^2}{4\pi} \frac{e^{-\mu_\rho \hat{r}_{ij}}}{\hat{r}_{ij}}$$

quark many body effects



Many-body effects on EOs

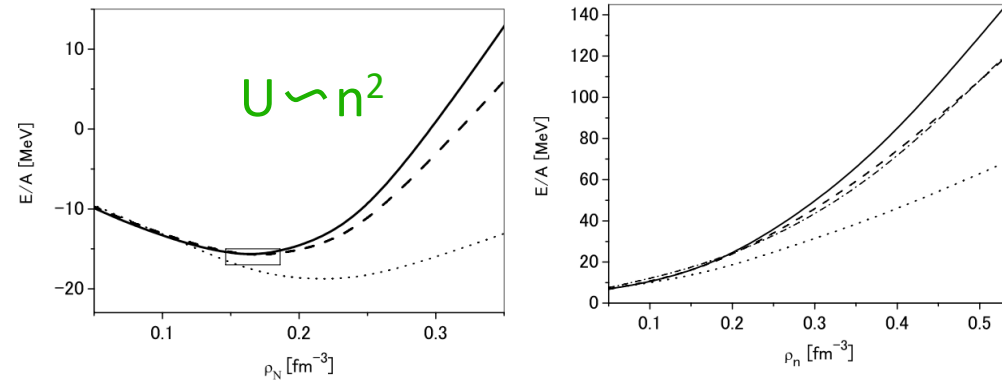
$$n^2 \sim (1/r)^6$$



$$U_{\text{SJM2}}(r; \rho_B) = V_r \rho_B (1 + c_r \rho_B / \rho_0) \exp[-(r/\lambda_r)^2]$$

introduced to be consistent with MR relations.

BHF with hyperons by Yamamoto, NY, Rijken (2022)



$$V_{eff}^{(N)}(\mathbf{x}_1, \mathbf{x}_2) = \rho_{NM}^{N-2} \int d^3x_3 \dots \int d^3x_N V(\mathbf{x}_1, \mathbf{x}_2, \dots, \mathbf{x}_N)$$

$$= g_P^{(N)} g_P^N \frac{\rho_{NM}^{N-2}}{\mathcal{M}^{3N-4} \pi \sqrt{\pi}} \left(\frac{m_P}{\sqrt{2}}\right)^3 \exp\left(-\frac{1}{2} m_P^2 r_{12}^2\right), (3)$$

$N=3,4$

introduced to be consistent with MR relations

and/or cross sections of nuclei.

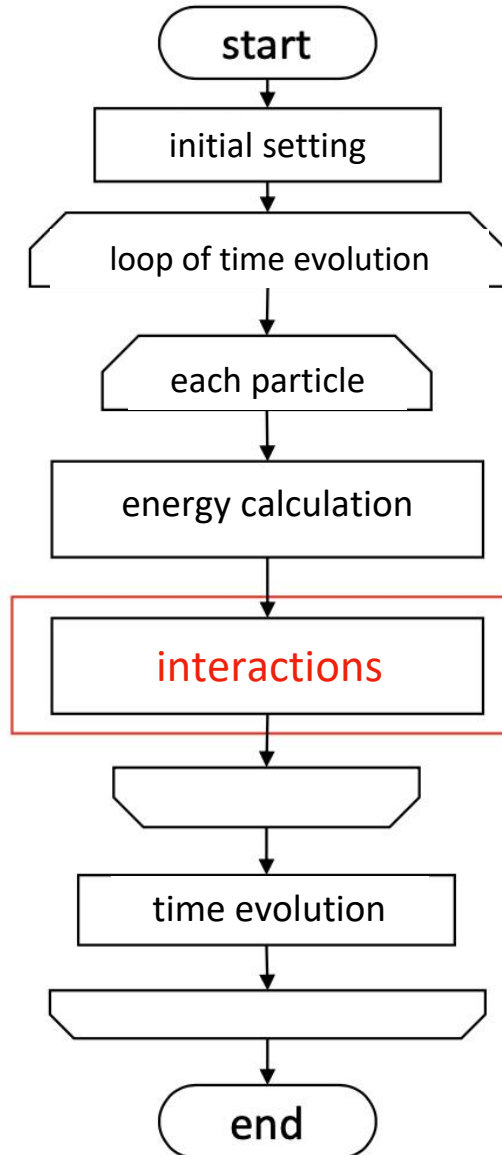
These examples are adopted to hadron interactions.

Why not to quark-quark interactions?

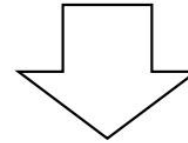
$$U_{qqq} \sim (1/r)^{1+\epsilon}$$

Parallel computings in MD

No money(GPUs), No study....



- The main part of calculations ($\sim 90\%$).
→ The main target to be improved.



- Super computer in JAEA
- parallel computings

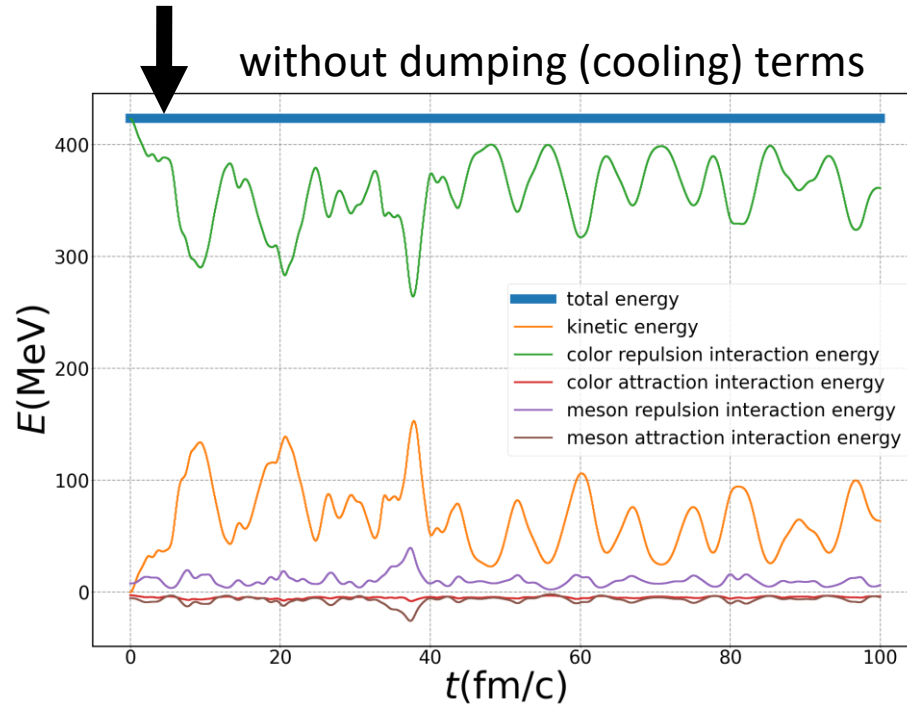


Device : HPE SGI 8600 in JAEA
CPU : Intel Xeon Gold 6428R
(3.0GHz, 35.75MB cache)X 2CPU
Core number per node : 48
GPU : NVIDIA Tesla V100 SX2 32GB memory
(FP64/GPU : 2560)x4GPU
Memory per node : 384 GB

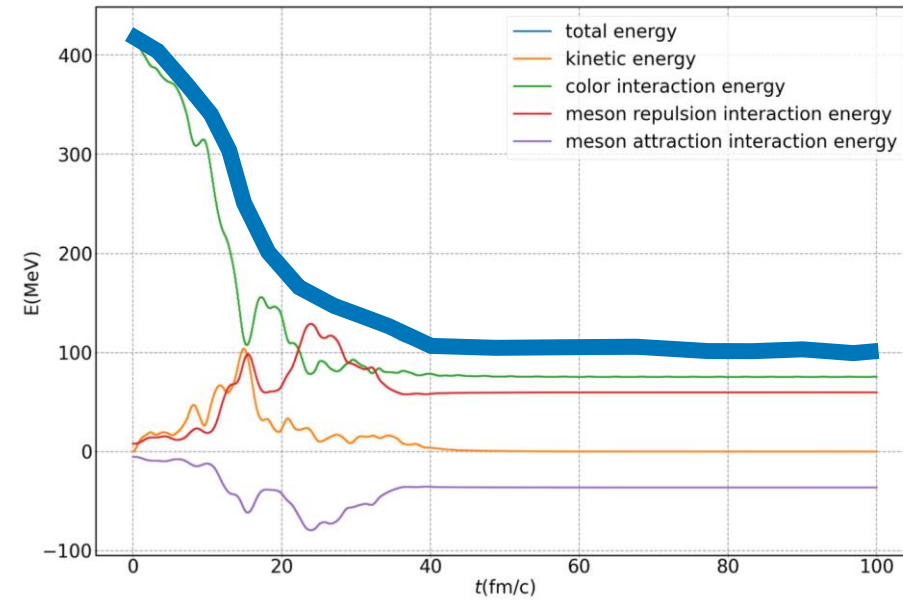
Energy conservation

as an accuracy check

total energy

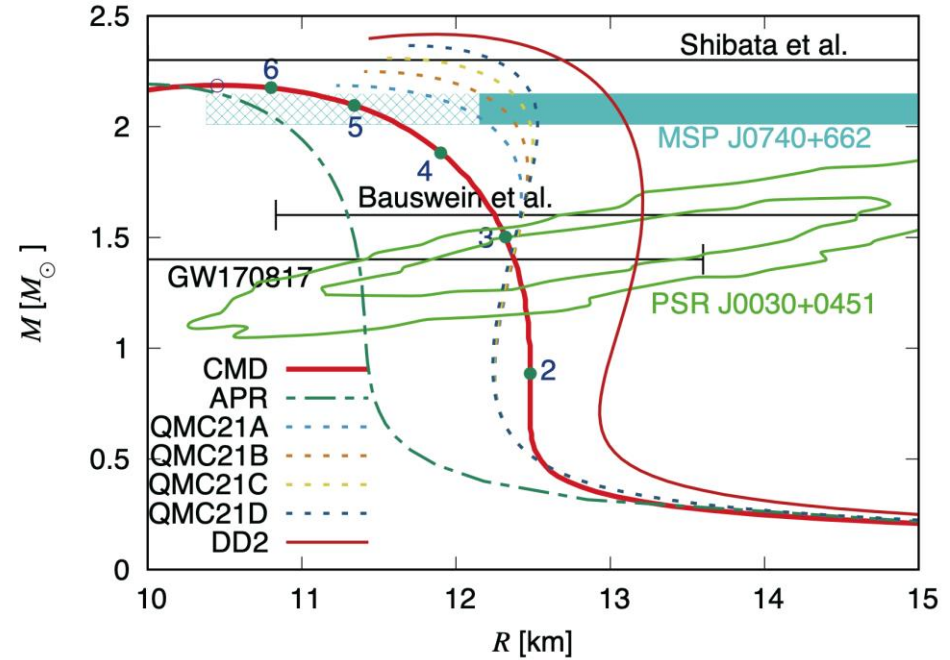
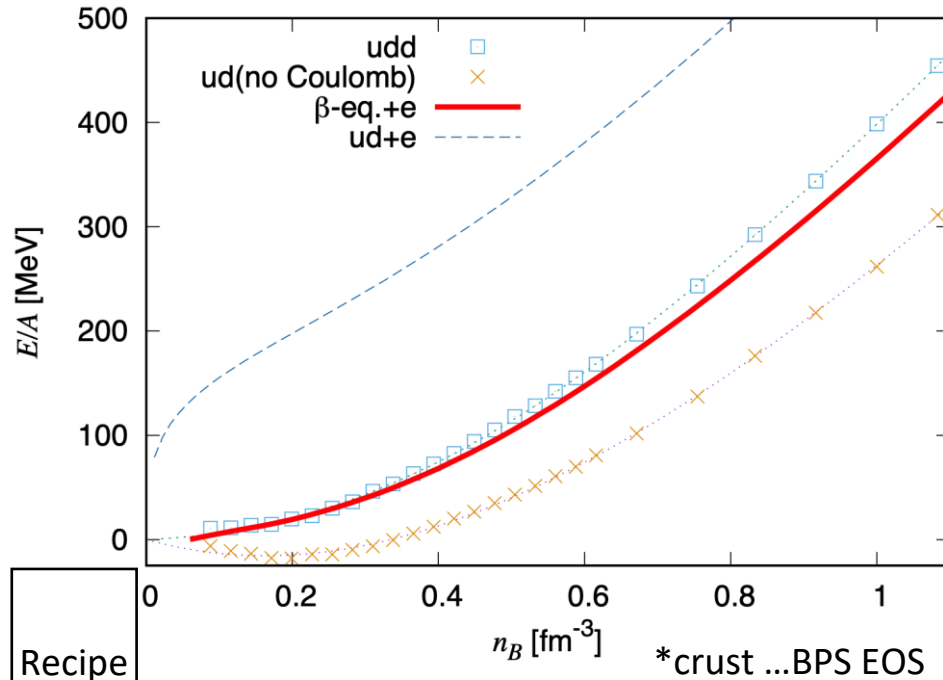


including dumping (cooling) terms



$$\dot{\mathbf{R}}_i = \frac{\partial H}{\partial \mathbf{P}_i} + \mu_R \frac{\partial H}{\partial \mathbf{R}_i},$$
$$\dot{\mathbf{P}}_i = -\frac{\partial H}{\partial \mathbf{R}_i} + \mu_P \frac{\partial H}{\partial \mathbf{P}_i},$$

EOS by Color-Molecular-dynamics



- ① We derive fitting formulae from numerical data points. (~ 1day for 1 parameter set)
- ② We obtain EOS using the formulae under beta equilibrium and charge neutrality conditions.

beta eq.

$$\mu_u + \mu_e = \mu_d,$$

$$\mu_p + \mu_e = \mu_n = \mu_u + 2\mu_d.$$

charge neutrality

$$en_{\text{ch}}(\mathbf{r}) \equiv \sum_{q=u,d,e} Q_q n_q(\mathbf{r})$$

$$en_{\text{ch}}(\mathbf{r}) = \sum_{i=n,p,e} Q_i n_i(\mathbf{r})$$

- ③ We check whether the EOSs are consistent with astrophysical constraints, and the nuclear experiments result.

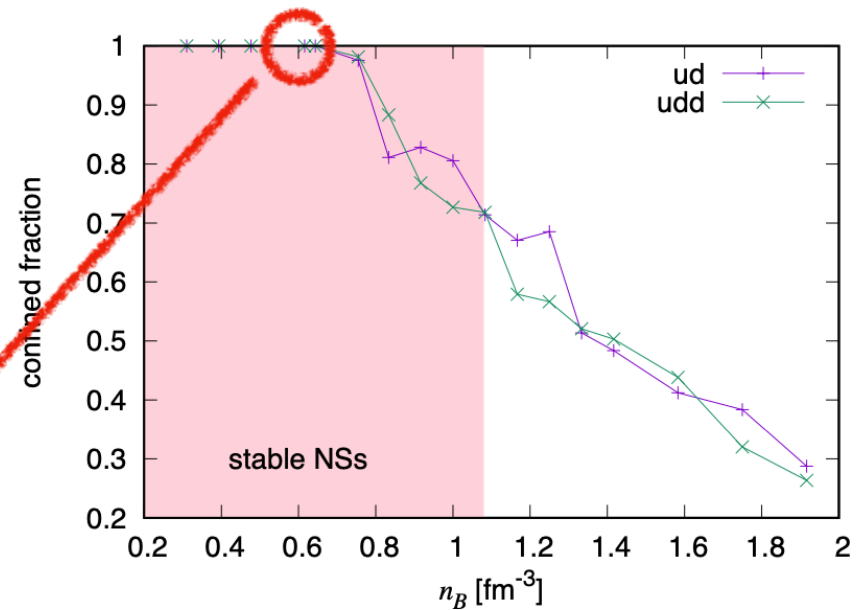
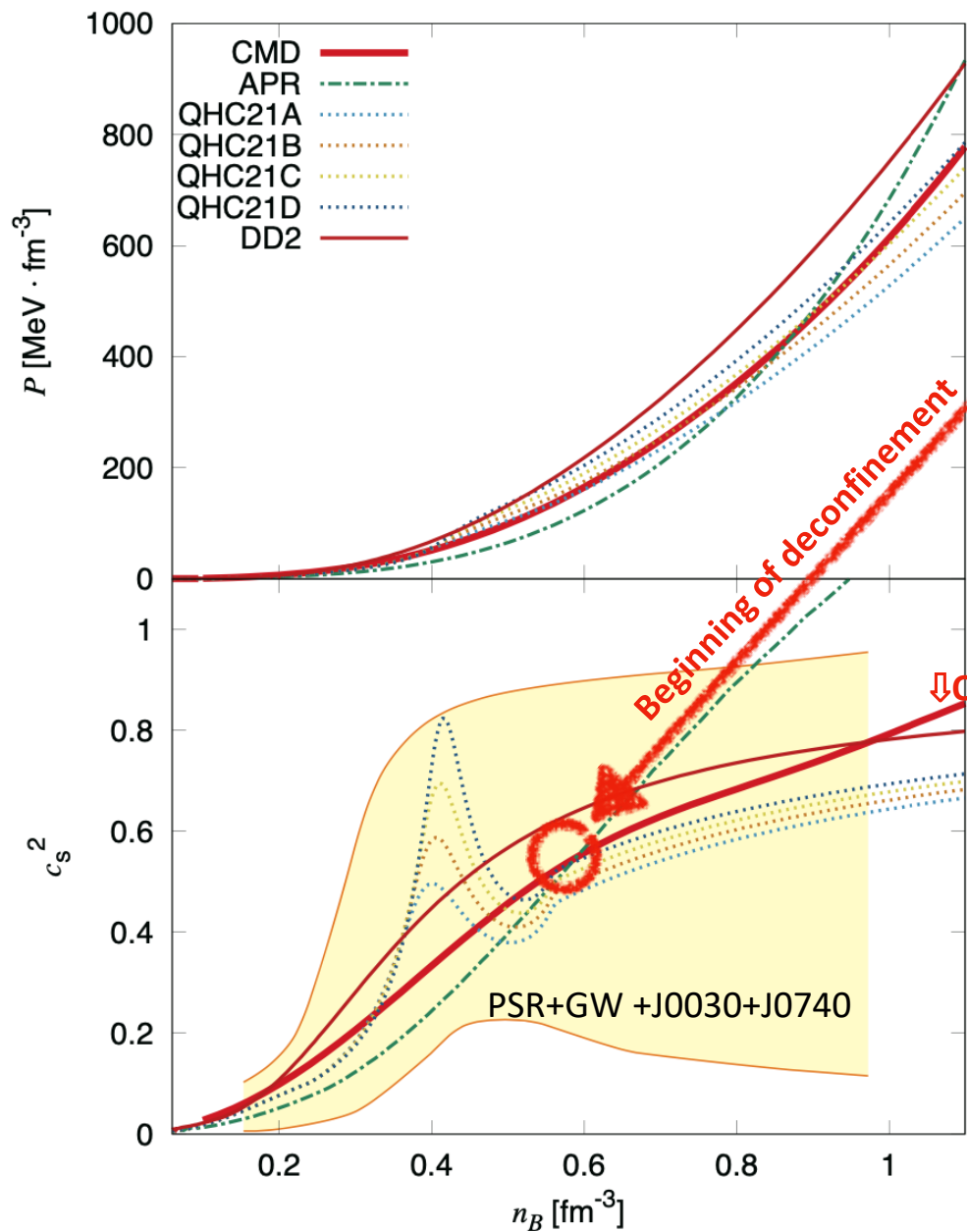
cf.) the above result

$$n_0=0.167\text{fm}^{-3}, S_0=-15.8\text{ MeV}, J=31.0\text{MeV}, L=74.2\text{MeV}, K=260\text{ MeV}, M_{\text{max}}=2.19\text{ Ms}, \Lambda_{1.4}=458, n_c=1.08\text{ fm}^{-3}$$

ref) Danielewicz et al., Science 298 (02) 1592: K = 167-300 MeV

try next parameter

Pressure & Sound velocity



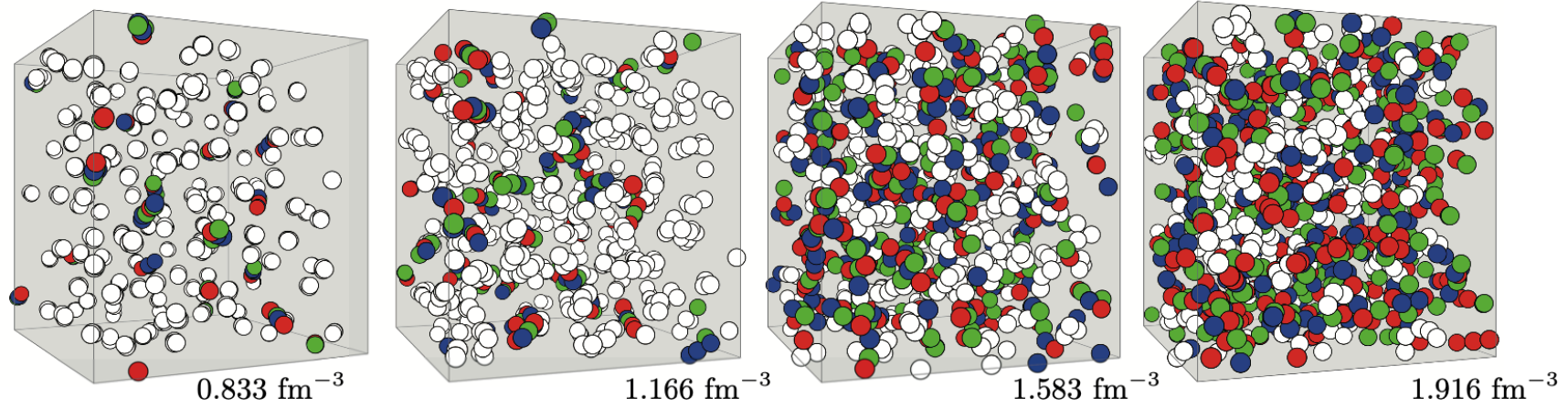
• The main component of NSs are hadron matter.

↓ Our result

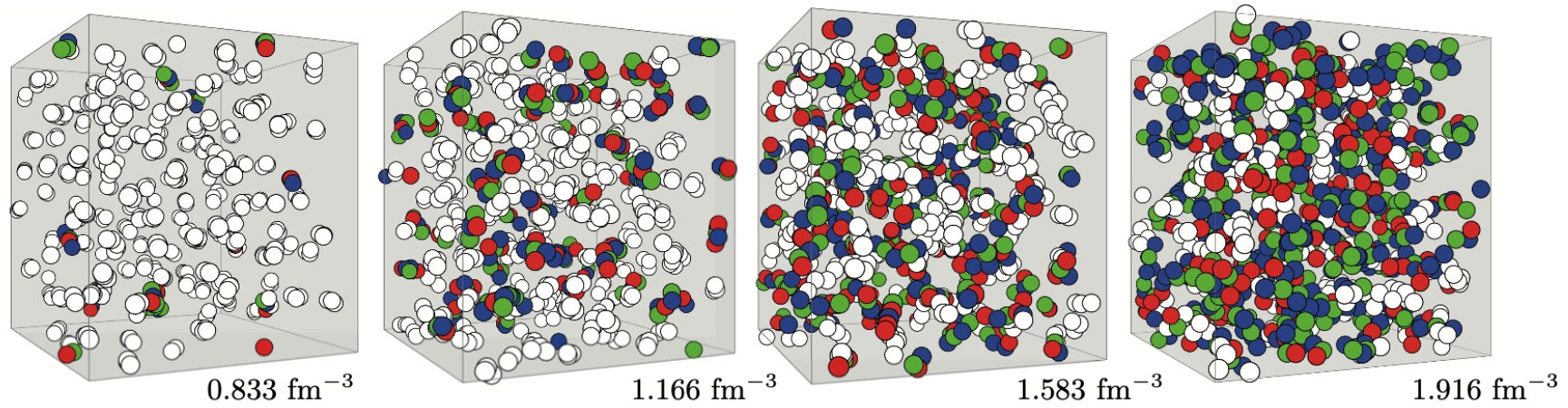
• The inflection point is the quark deconfinement origin.

• The peak of sound speed appears higher density than the maximum density of NSs in our models.

ud matter



The perspectives for *ud* matter depended on density. Each color corresponds to the color's internal degree of freedom for each quark: the white color balls represent the quarks in the baryon state, while red, blue, and green ones do in the deconfined quark matter.

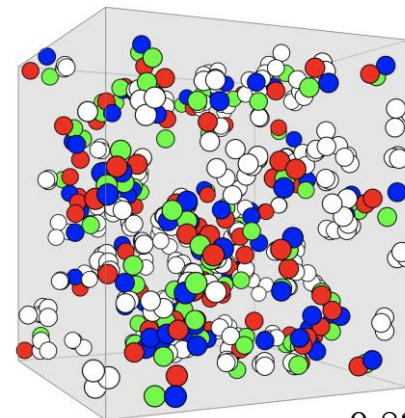
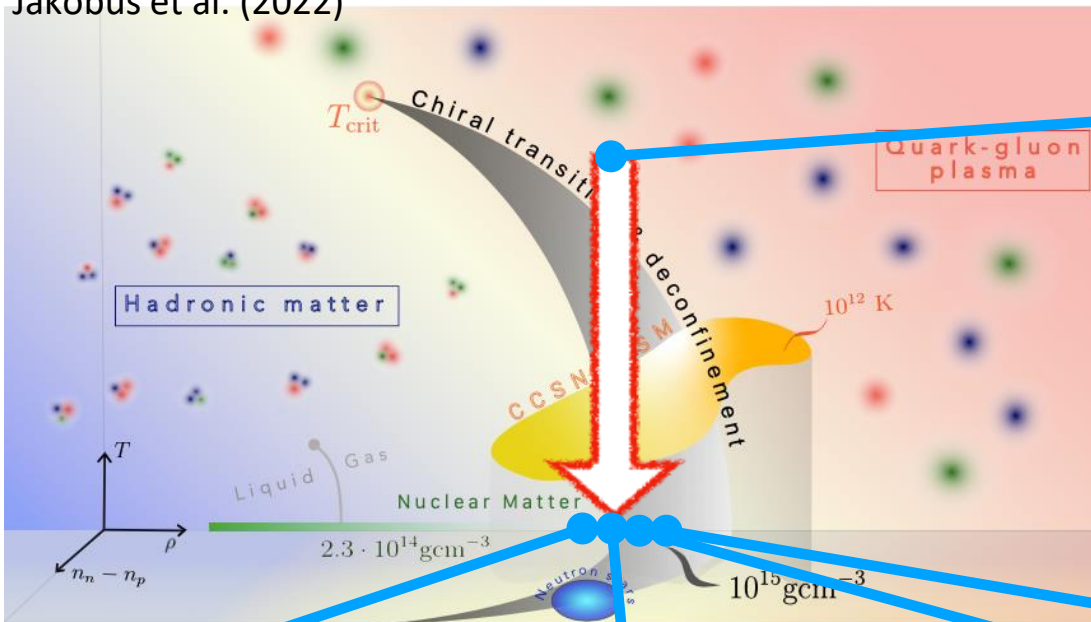


←→
stable NSs $n_c = 1.08 \text{ fm}^{-3}$

uudd matter.

Phase diagram

Jakobus et al. (2022)

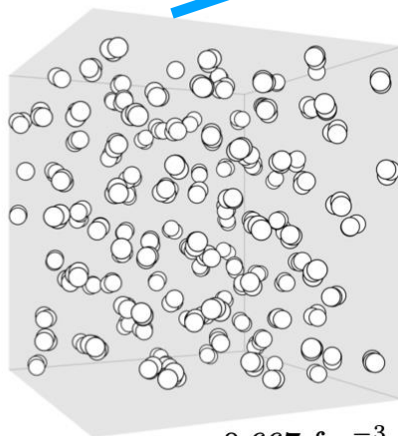


0.834 fm^{-3}

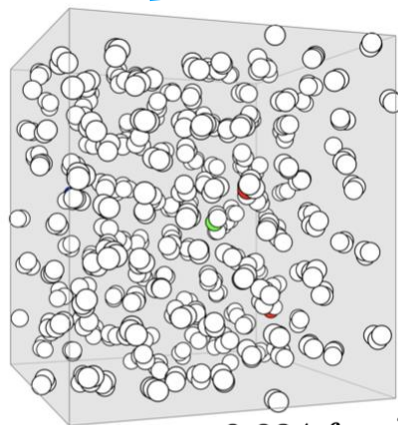
$$\dot{\mathbf{R}}_i = \frac{\partial H}{\partial \mathbf{P}_i} + \mu_R \frac{\partial H}{\partial \mathbf{R}_i},$$

$$\dot{\mathbf{P}}_i = -\frac{\partial H}{\partial \mathbf{R}_i} + \mu_P \frac{\partial H}{\partial \mathbf{P}_i},$$

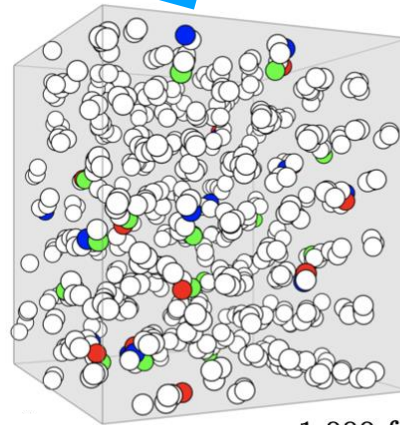
pure symmetric matter



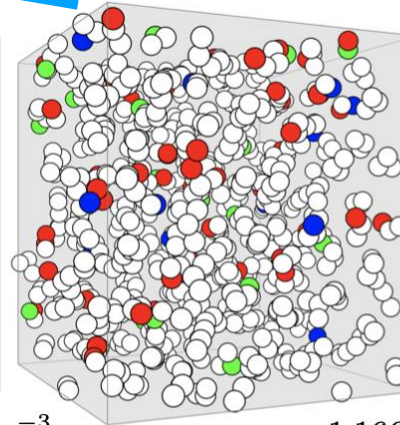
0.667 fm^{-3}



0.834 fm^{-3}

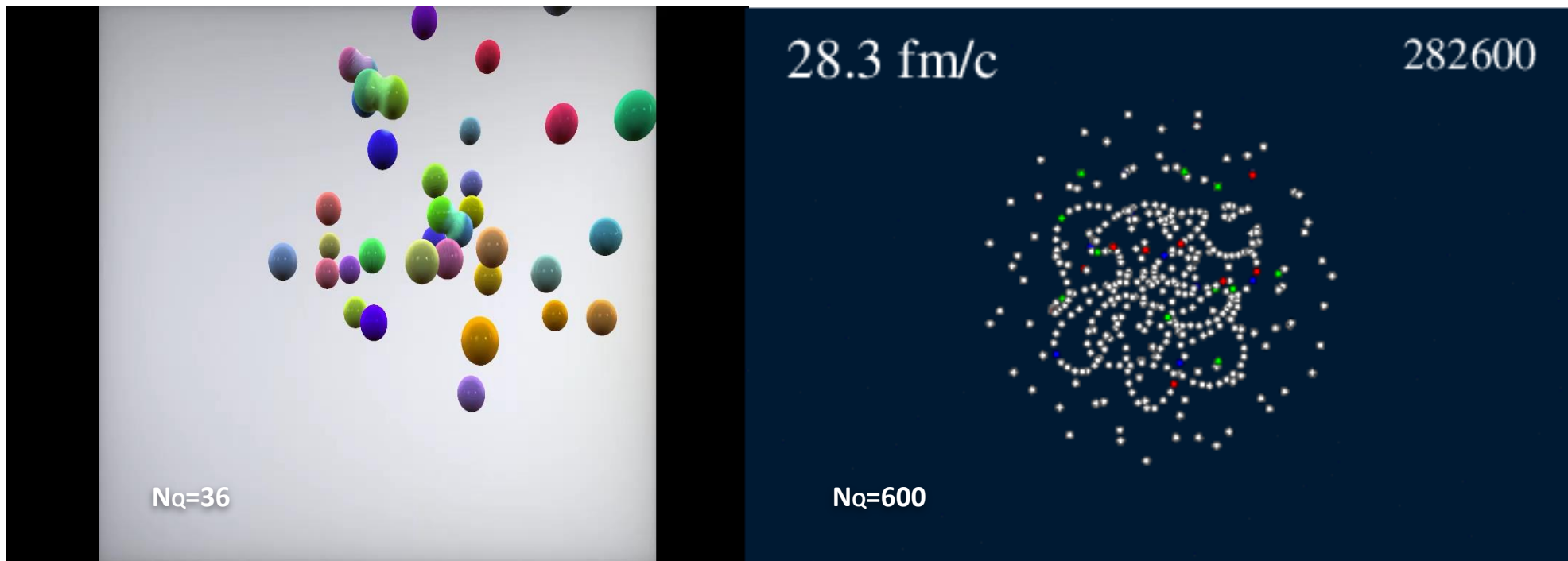


1.000 fm^{-3}

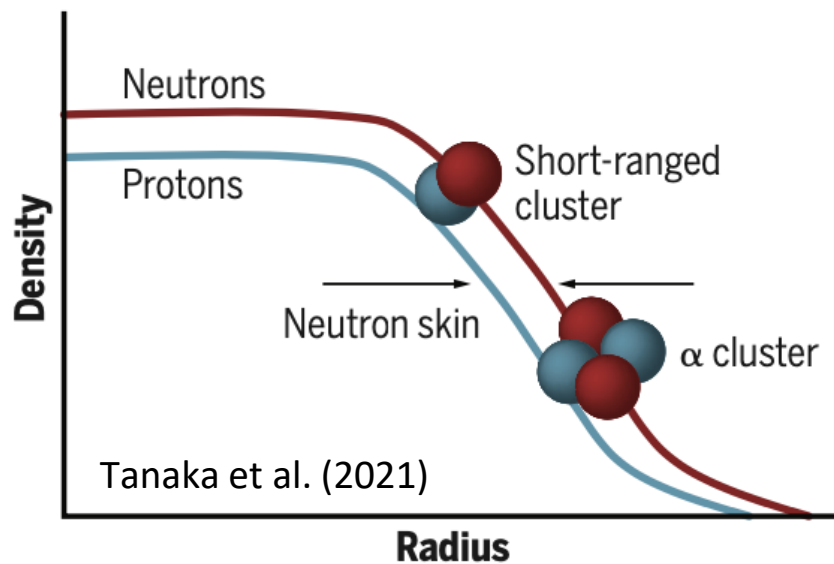


1.166 fm^{-3}

Finite system consistent with finite system



Nucleon density in neutron-rich nuclei



RMF + alpha cluster(local correlation) neutron skin change 10-40%
 "DD2" Typel, Ropke, Klahn, Blaschke, Wolter, PRC. 81, 015803 (2010).

Typel, PRC.89,064321(2014).

| Theoretical cross sections (nb) | Effective number of α clusters | Theoretical Δr_{np} without α (fm) | Theoretical Δr_{np} with α (fm) | Relative Δr_{np} change (%) |
|---------------------------------|---------------------------------------|---|--|-------------------------------------|
| 0.160 | 0.3876 | 0.0495 | 0.0277 | -44 |
| 0.127 | 0.3304 | 0.0843 | 0.0580 | -31 |
| 0.095 | 0.2668 | 0.1179 | 0.0912 | -23 |
| 0.065 | 0.1958 | 0.1505 | 0.1275 | -15 |

Color magnetic interaction and baryon mass

interactions with colors

$$\hat{V}_{\text{color}} = \frac{1}{2} \sum_{i=1, j \neq i}^n \left(- \sum_{a=1}^8 \frac{\lambda_i^a \lambda_j^a}{4} \left(K \hat{r}_{ij} - \frac{\alpha_s}{\hat{r}_{ij}} \right) \right)$$

$$V_{ij}^{CS} = \frac{\kappa'}{m_i m_j r_{0ij}^2} \frac{1}{r_{ij}} e^{-(r_{ij}/r_{0ij})^2} \lambda_i^c \lambda_j^c \uparrow \text{ or } \downarrow$$

$$r_{0ij} = (\alpha + \beta \mu_{ij})^{-1}. \quad \mu_{ij} = m_i m_j / (m_i + m_j)$$

Aaron et al. EPJA 56,93(2020)

| α_s | κ' | K | α | β | $m_{u,d}$ | m_s | L |
|------------|-----------|---------------------|------------------|---------|-----------|-------|-------|
| 1.25 | 0.5 | 750 | 2.1 | 0.552 | 0.362 | 0.538 | 0.346 |
| | | MeVfm ⁻¹ | fm ⁻¹ | | GeV | GeV | fm |

~ 1/(2m)

Akimura et al. EPJA 25,405(2005) etc.

Optimized in this study.

2-body spin correlations

$$\langle \frac{\sigma_i}{2} \cdot \frac{\sigma_j}{2} \rangle = \frac{1}{4} (\uparrow\uparrow), -\frac{3}{4} (\uparrow\downarrow)$$

| (I, S) | ($\frac{1}{2}, \frac{1}{2}$) | ($\frac{1}{2}, \frac{3}{2}$) | (0, $\frac{1}{2}$) | (1, $\frac{1}{2}$) | (1, $\frac{3}{2}$) | ($\frac{1}{2}, \frac{1}{2}$) | ($\frac{1}{2}, \frac{3}{2}$) |
|--------|--------------------------------|--------------------------------|---------------------|---------------------|---------------------|--------------------------------|--------------------------------|
| | N,P | Δ | Λ | Σ | Σ^* | Ξ | Ξ^* |
| M_B | 0.90 6 | 1.24 5 | 1.075 | 1.07 5 | 1.41 5 | 1.21 7 | 1.58 4 |
| Expt. | 0.938 | 1.232 | 1.115 | 1.189 | 1.382 | 1.315 | 1.532 |



2-body spin correlations consistent with 3-body spin correlations

$$\langle \frac{\sigma_i}{2} \cdot \frac{\sigma_j}{2} \rangle = \frac{1}{4} (\uparrow\uparrow), -\frac{1}{2} (\uparrow\downarrow)$$

| (I, S) | ($\frac{1}{2}, \frac{1}{2}$) | ($\frac{1}{2}, \frac{3}{2}$) | (0, $\frac{1}{2}$) | (1, $\frac{1}{2}$) | (1, $\frac{3}{2}$) | ($\frac{1}{2}, \frac{1}{2}$) | ($\frac{1}{2}, \frac{3}{2}$) |
|--------|--------------------------------|--------------------------------|---------------------|---------------------|---------------------|--------------------------------|--------------------------------|
| | N, P | Δ | Λ | Σ | Σ^* | Ξ | Ξ^* |
| M_B | 0.938 | 1.233 | 1.115 | 1.177 | 1.379 | 1.328 | 1.531 |
| Expt. | 0.938 | 1.232 | 1.115 | 1.189 | 1.382 | 1.315 | 1.532 |

others

quark-meson coupling

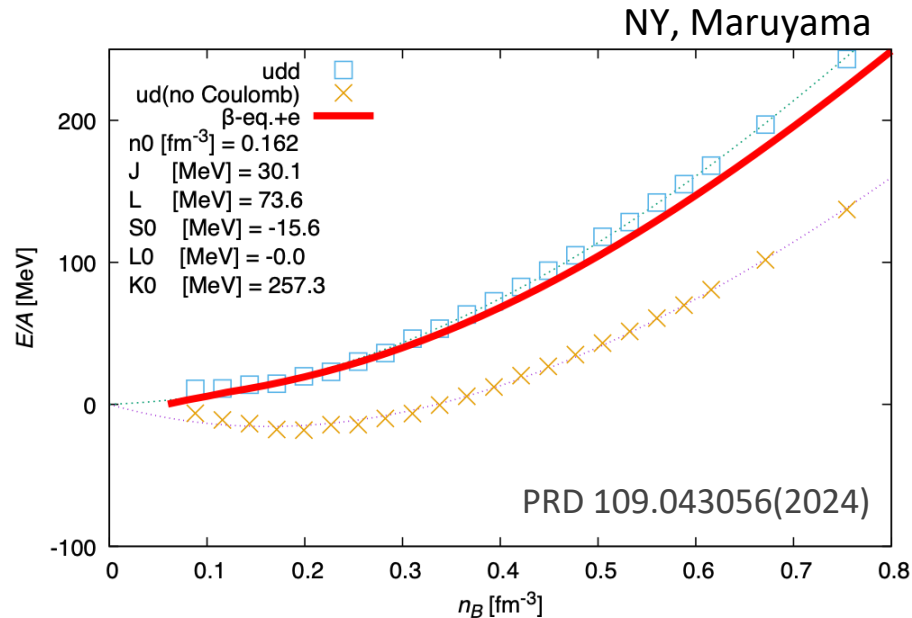
$$V_{\text{meson}}(r) \equiv -\frac{g_{\sigma q}^2}{4\pi} \frac{e^{-\mu_\sigma r_{ij}}}{r_{ij}} + \frac{g_{\omega q}^2}{4\pi} \frac{e^{-\mu_\omega r_{ij}}}{r_{ij}} + \frac{\sigma_i^3 \sigma_j^3}{4} \frac{g_{\rho q}^2}{4\pi} \frac{e^{-\mu_\rho \hat{r}_{ij}}}{\hat{r}_{ij}}$$

pauli interaction

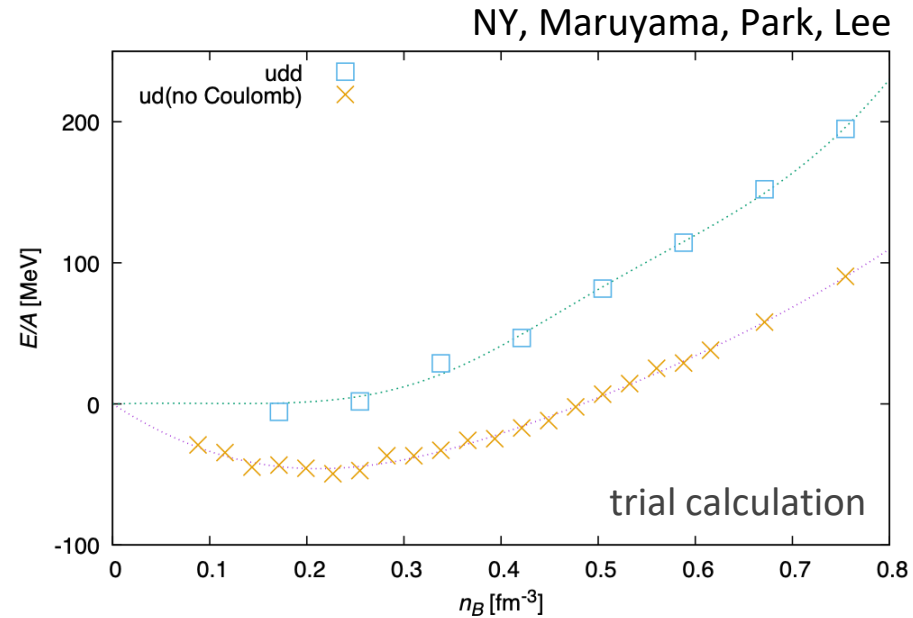
$$\langle V_{\text{pauli}}(r) \rangle \equiv \frac{C_p}{(q_0 p_0)^3} \exp \left[-\frac{(\mathbf{R}_i - \mathbf{R}_j)^2}{2q_0^2} - \frac{(\mathbf{P}_i - \mathbf{P}_j)^2}{2p_0^2} \right] \delta_{\chi_i \chi_j}$$

Color magnetic interaction and EOS

without color-magnetic interaction



with color-magnetic interaction



$$S_i = \begin{pmatrix} 1 \\ 0 \end{pmatrix} \text{ or } \begin{pmatrix} 0 \\ 1 \end{pmatrix} \longrightarrow S_i = \begin{pmatrix} e^{-i\beta_i^{(s)}} \cos \alpha_i^{(s)} \\ e^{i\beta_i^{(s)}} \sin \alpha_i^{(s)} \end{pmatrix}$$

$$V_{ij}^{CS} = \frac{\kappa'}{m_i m_j r_{0ij}^2} \frac{1}{r_{ij}} e^{-(r_{ij}/r_{0ij})^2} \lambda_i^c \lambda_j^c \sigma_i \cdot \sigma_j,$$

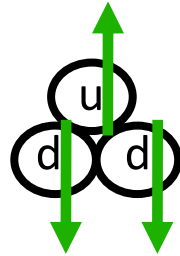
time dependent

Color magnetic interaction and spins

NY, Maruyama, Park, Lee

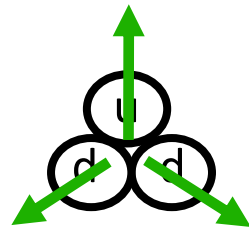
3-quark system

$$\langle \frac{\sigma_i}{2} \cdot \frac{\sigma_j}{2} \rangle = \frac{1}{4} (\uparrow\uparrow), -\frac{3}{4} (\uparrow\downarrow)$$

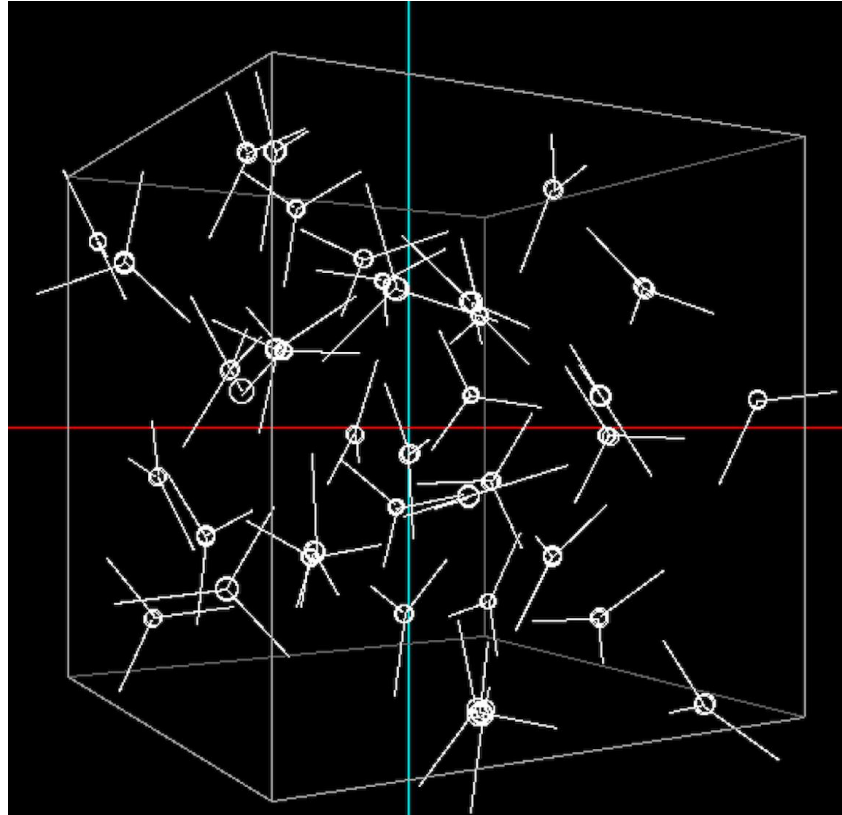


Large N-quark system

$$\langle \frac{\sigma_i}{2} \cdot \frac{\sigma_j}{2} \rangle = \frac{1}{4} (\uparrow\uparrow), -\frac{1}{4} (\uparrow\downarrow)$$



Mercedes-Benz



Around saturation density
with periodic boundary (infinite system)

Physical properties by MD

We can obtain physical quantities
by Green-Kubo formula.
(1st. order of fluctuation)

$$\alpha = \int_0^{\infty} \langle \dot{U}(t) \dot{U}(0) \rangle dt.$$

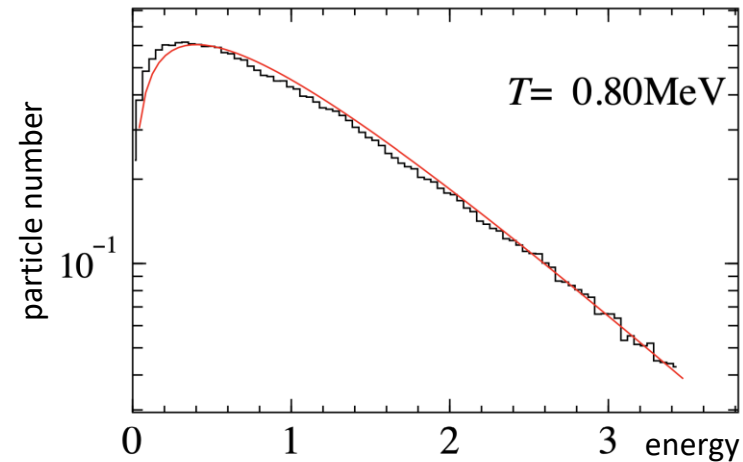
e.g. thermal conductivity λ

$$\alpha = VT^2\lambda,$$

$$U_x(t) = \sum_{i=1}^N x_i(t) E_i(t),$$

$$\dot{U}_x(t) = \frac{d}{dt} \sum_{i=1}^N x_i(t) E_i(t).$$

Statistical temperature from CMD is
consistent with theoretical distribution.



→(Proto)Neutron Star coolings / evolutions

Evolution of (Proto)Neutron Stars

Neutron Star evolution:

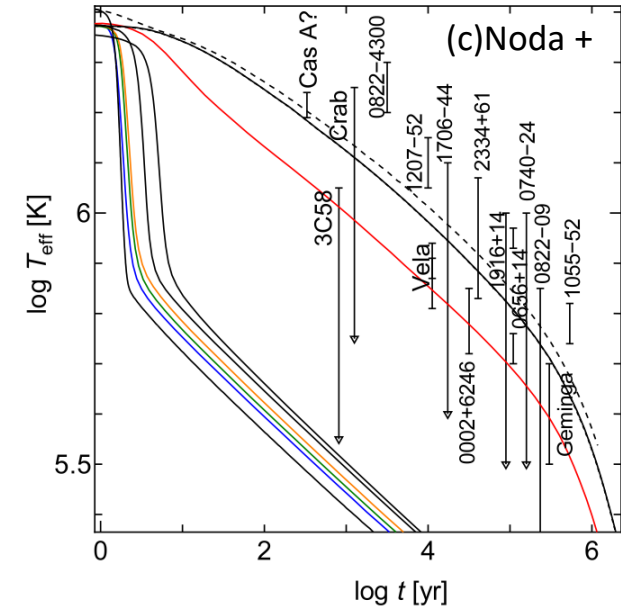
$$c_v e^\Phi \frac{\partial T}{\partial t} + \nabla \cdot (e^{2\Phi} \mathbf{F}) = e^{2\Phi} Q$$

heat capacity

flux (thermal conductivity)

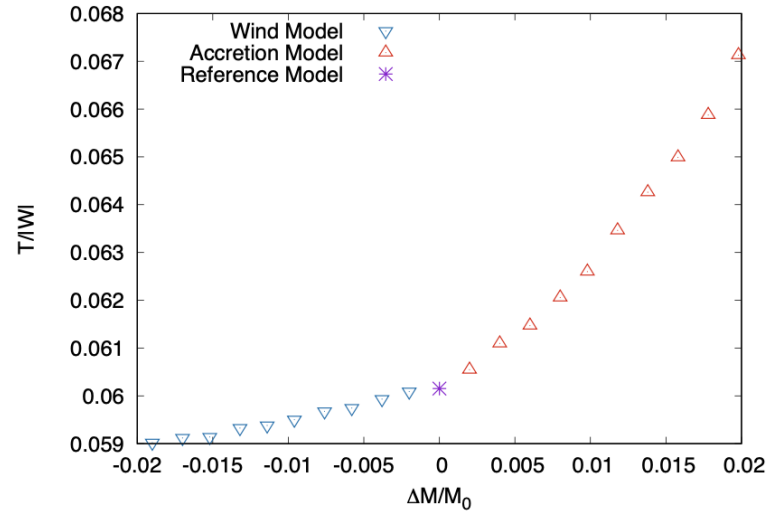
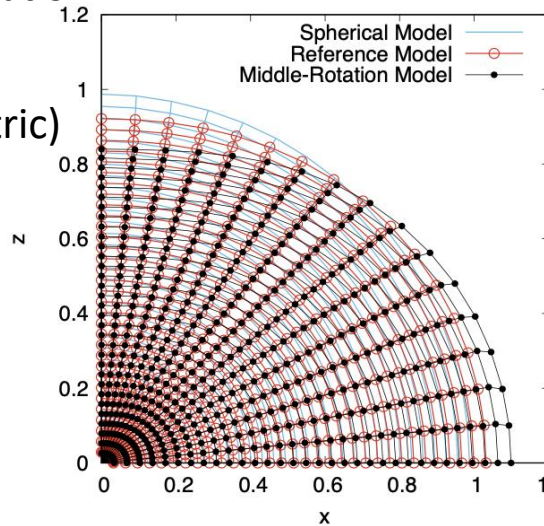
thermal diffusion eq.

cooling rate (neutrino) + heating rate (magnetic field)



Toward Proto Neutron Star evolution:

- hydrostatic equilibria in GR
 - Lagrange scheme (axisymmetric)
- +
- on going ...
- energy eq.
 - neutrino transports



Summary and Discussion

- We present CMD results, which is from QCD to neutron stars (hadron+quarks)
- EOS (MR relation) constraints
 - Low density ← nuclear experiments
 - High density ← astrophysical observations
- As the results, our CMD simulations provide a neutron star (NS) EoS.
- We find cross over deconfinement.
 - GW, Supernovae... ← Finite temperature behavior
- We need more realistic set up: relativistic effects, strangeness effects, vacuum effects.
- Now, we focus on CMD with Color-magnetic interactions.
- Our CMD will provide thermal properties for NS evolution in the future.